Advances in Structural Engineering

An International Journal

CONTENTS

Advances in Structural Engineering Volume 8 Number 6 December 2005

Advances in Structural Engineering

An International Journal

ISSN 1369-4332

Editor-in-Chief
Professor J. G. Teng
The Hong Kong Polytechnic University

Volume 8 Number 6 December 2005

A Multi-Science Publication

Base-isolated Building with Asymmetries due to the Isolator Parameters

Vasant A. Matsagar and R.S. Jangid*

Department of Civil Engineering, Indian Institute of Technology Bombay, Powai, Mumbai, India

(Received: 3 March 2005; Received revised form: 22 July 2005; Accepted: 5 August 2005)

Abstract: the effects of torsional coupling, due to isolator parameters, on the seismic response of base-isolated buildings are presented. The isolated building is modelled as a single-storey structure mounted on different isolation devices such as elastomeric and sliding systems involving non-linear restoring forces. The governing equations of motion for the uncoupled and torsionally coupled system are derived and solved in time domain by Newmark's method of integration to obtain lateral-torsional displacement response. The displacement response of the isolated system with different combinations of structural configurations, isolation systems and the ratio of uncoupled torsional to lateral frequency of the system is investigated. A comparison of the response of the torsionally coupled base-isolated building is made with the corresponding response obtained from torsionally uncoupled base-isolated building. In addition, a parametric study is conducted to observe the effect of superstructure flexibility on the displacements in torsionally coupled base-isolated building. The eccentricities arising due to the asymmetries in the isolation stiffness and/ or yield strength of the isolators are compared with the eccentricity in the system as specified by the Uniform Building Code (UBC 1997). It is observed that the torsional coupling arising due to the dissimilarity in the isolator properties considerably influences the seismic response of the base-isolated building. Effects of superstructure eccentricity are found diminishing when the isolation eccentricities exist. The design bearing displacement suggested by the UBC static formula incorporating accidental torsion is found conservative for the isolation eccentricities arising due to the dissimilarity amongst the isolators.

Key words: asymmetry, base isolation, couple, earthquake, elastomeric, seismic, sliding, torsion.

1. INTRODUCTION

The seismic isolation has emerged as a potential strategy in preventing damages to the buildings and sensitive equipments housed within it during severe earthquakes. The basic concept of isolation is to detach the building from ground, instead of the conventional techniques of strengthening the structural members. The isolation devices essentially have two important roles to play: providing horizontal flexibility and serve as energy dissipation mechanism. The flexibility of the isolation system results in lengthening of the fundamental time period of the building, shifting it away from the region of dominant earthquake frequency contents, whereas the energy absorbing capacity increases due to the isolation damping.

*Corresponding author. Email address: rsjangid@civil.iitb.ac.in; Fax: +91 22 2576 7302; Tel: +91 22 2576 7346.

Most of the research contribution (Kelly 1986; Jangid and Datta 1995a) on seismic isolation of structures deals with two-dimensional (2-D) idealization, which is strictly valid for the symmetric structures or those with very small eccentricity or torsionally very stiff. However, 2-D modelling lead to unrealistic results for the structures with asymmetric plans, therefore a three-dimensional (3-D) analysis of such systems is resorted to obtain the accurate design displacements and forces. Most of the real buildings are asymmetrical because of their mass and/ or stiffness distributions contrary to an ideal 2-D system. The structural irregularities such as irregular distribution of mass, stiffness or strength in their floor plan leads to coupling of the displacements in lateral and torsional directions. The buildings excited by the earthquake ground motions undergo lateral as well as torsional motions, if the centers of structural mass and stiffness do not coincide at the floor level. Such a torsional coupling in case of the base-isolated buildings may lead to substantial increase in its seismic response, which essentially depends upon properties of the building and the isolation system utilized. Several base isolation systems have been developed (Jangid and Datta 1995a), categorized broadly as elastomeric bearings and sliding systems adopted effectively in seismic isolation of the buildings. The bearings are essentially orthotropic in nature therefore it has same natural frequencies in the lateral and longitudinal directions of the system. However, when the building is torsionally coupled due to the system properties, a strong coupling of responses in the three principal directions may occur when the torsional frequency is closer to the two lateral frequencies. Such torsional coupling occurs, especially in case of base-isolated buildings, if the eccentricity between center of mass (CM) and center of rigidity (CR) exists at superstructure and/ or at the isolation level. The building may experience highly increased response when the line joining CM and CR is perpendicular to the direction of earthquake excitation.

The building codes (UBC 1997; IBC 2000) recommend that, the location of the CR with respect to the CM should be selected in such a way as to provide the worst-case displacement while calculating the displacements due to the torsion. The codes recommend consideration of the accidental eccentricity in design even if the building is symmetric. Hence, it is essential to study the behavior of base-isolated structures under torsionally coupled conditions. The investigations made in the past on the torsional response of base-isolated structures are reviewed here. The effectiveness of bi-linear hysteretic base isolation systems in an asymmetric single-storey structure subjected to the bi-directional earthquake excitation was studied by Lee, (1980). It was concluded that the structural torque decreases as the isolation system eccentricity decreases and the superstructure eccentricity has meager effect on the torsional response. A modal analysis was presented by Pan and Kelly (1983) for the dynamic analysis of the base-isolated raft on elastomeric systems with eccentricities, showing effects of torsional coupling. The lateral displacements were shown reduced with the presence of asymmetries and delineated need to predict properly the corner displacements in the asymmetric base-isolated structures to avoid impact on the adjacent structures. The alternative designs of bi-linear base isolation systems were proposed by Eisenberger and Rutenberg (1986) for different multi-storey buildings. It was recommended that matching of the centers of rigidity and yield force of the base isolation system with the center of mass of the superstructure, reduces torsional effects. Torsion in the multi-storey base-isolated structures under bi-directional earthquakes, including the strength and other eccentricities of the various types of isolation systems was studied by Nagarajaiah *et al.* (1991, 1993a, 1993b); Reinhorn *et al.* (1994); and Tsopelas *et al.* (1994). These investigations concluded that the eccentricities at the isolation level as well as at the superstructure affects the seismic response of the structures and the increased flexibility of the superstructure calls upon the higher mode effects on the lateral-torsional response of the base-isolated structures. The non-linear response of torsionally coupled base-isolated structures with different isolation systems was studied by Jangid and Datta (1994a, 1994b, 1995b, 1995c); and Jangid (1996). In these studies, it was concluded that the eccentricity at the isolation level decreases the effectiveness of isolation for torsional deformation, increases the base displacements and marginally decreases the superstructure displacement perpendicular to the direction of eccentricity. However, the eccentricity of the superstructure and the angle of incidence of earthquake excitation have insignificant influence on the response. The seismic response of torsionally coupled multi-storey structures with different isolators under bi-directional subduction earthquakes of the Mexican Pacific Coast was studied by Tena-Colunga *et al.* (1997); Tena-Colunga and Gomez-Soberon (2002). These studies also confirmed that the torsional coupling reduces the effectiveness of isolation whereas the superstructure properties affect the response considerably. A simplified and approximate Raleigh-Ritz procedure was developed by Ryan and Chopra (2002) for the base-isolated structure with asymmetries at the superstructure and isolation level, and compared with the prevailing exact methods. It was observed that the proposed method yielded results closely matching with the exact solutions when eccentricities exist. A review was presented by Gavin *et al.* (2003) on the past studies made on asymmetric base-isolated structures with passive control systems; and the effects of provision of semi-active hydraulic damper in a torsionally coupled multi-storey base-isolated building were discussed. Thus in most of the publications, it has been emphasized that the torsional coupling has a significant effect on the behavior of base-isolated buildings and it has to be duly considered. However, the eccentricities arising due to dissimilarity in the isolation stiffness or isolator yield strength are not addressed so far exclusively. In this context, it is important to study the performance of different isolation systems used for isolation of a torsionally coupled building and the effects of eccentricity in the restoring force provided by the isolation systems at the isolation level.

The objective of this study is to identify important system parameters influencing on the lateral-torsional response of the torsionally coupled systems. The specific objectives of the present study are to (i) compare the performance of elastomeric and sliding isolation systems under torsional coupling in light of the static design rule specified by the UBC; (ii) study the influence of eccentricities arising because of variation in the isolation stiffness and the yield strength; and (iii) examine the effect of superstructure flexibility on the torsional response of the base-isolated buildings.

2. STRUCTURAL MODEL

In this study, the base-isolated building is idealized as a single-storey structure with masses lumped at the top-deck and at the base-raft as shown in Figure 1. The top-deck of dimensions $B \times D$ in plan is supported by mass-less, axially inextensible columns. The base-raft of dimensions $B \times D$ in plan is mounted on the various types of seismic isolators. The CR of the columns may not coincide with the CM of the top-deck and the CR provided by the restoring forces in the isolation systems

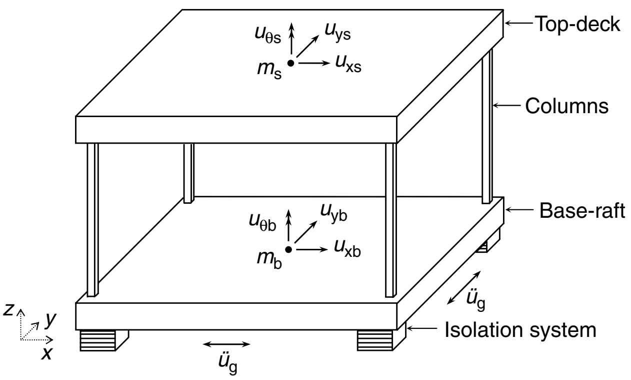

Figure 1. 3-D base-isolated single-storey building model

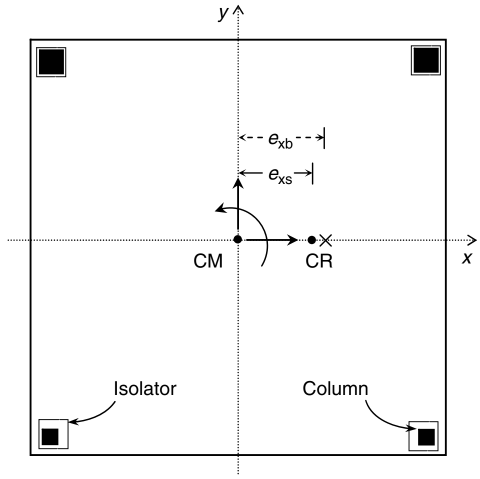

Figure 2. Various eccentricities in the asymmetric base-isolated building

at base-raft may not coincide with the CM of the base-raft as shown in Figure 2; on account of manufacturing/construction defects and faults. Hence, the main sources of asymmetries in base-isolated building considered here are: (i) due to the variation in the stiffness provided by columns, k_{xi} and k_{yi} at the superstructure, labelled as superstructure eccentricity; (ii) due to the variation in the stiffness, k_{xbj} and k_{ybj} of the isolation systems; and (iii) due to the variation in the yield strength, f^y or friction coefficient, μ in the elastomeric or sliding isolation systems, respectively. The eccentricities arising at the base-raft are labelled as isolation eccentricities. The eccentricities arising due to the unequal distribution of mass need not be considered once the eccentricity of CR is expressed with reference to CM. As suggested in the past studies (Ryan and Chopra 2004) that the response of a two-way asymmetric system is predicted accurately by a one-way asymmetric model with the same magnitude of eccentricity hence, the uni-directional eccentricities in the *x*-direction are considered herein for both the superstructure and isolation eccentricities (Figure 2). Therefore, the torsional coupling of displacements will occur for the earthquake ground acceleration in the *y*-direction. The two degrees-of-freedom in which coupling occurs are the lateral displacement, u_y and the torsional displacement, u_θ in the system subjected to ground motion in *y*-direction. The motion of the building in the *x*-direction is uncoupled with torsion and can be considered separately, as interacting (Jangid and Datta 1995b) with the lateral displacement in *y*-direction.

3. ASYMMETRIES AT THE SUPERSTRUCTURE

If k_{xi} and k_{yi} represent the lateral stiffness of *i*th column in *x*- and *y*-directions, respectively then

$$K_{\mathrm{xs}} = \sum_i k_{\mathrm{xi}} \text{ and } K_{\mathrm{ys}} = \sum_i k_{\mathrm{yi}} \tag{1}$$

are the total lateral stiffness of the superstructure in the x- and y-directions, respectively.

The torsional stiffness of the superstructure defined about the vertical axis passing through the CM of the top-deck is given by

$$K_{\theta\mathrm{s}} = \sum_i \left(k_{\mathrm{xi}}\ y_i^2 + k_{\mathrm{yi}}\ x_i^2 \right) \tag{2}$$

where x_{i} and y_{i} denote the x- and y- coordinates of the i^{th} column with respect to the CM of the top-deck, respectively. The torsional stiffness of each individual column cross-section is negligible and therefore ignored. The uncoupled frequency parameters of the system are defined as follows

$$\omega_{\mathrm{xs}} = \sqrt{\frac{K_{\mathrm{xs}}}{m_{\mathrm{s}}}},\ \omega_{\mathrm{ys}} = \sqrt{\frac{K_{\mathrm{ys}}}{m_{\mathrm{s}}}} \text{ and } \omega_{\theta\mathrm{s}} = \sqrt{\frac{K_{\theta\mathrm{s}}}{m_{\mathrm{s}} r_{\mathrm{s}}^2}} \tag{3}$$

where m_{s} and r_{s} are the mass and radius of gyration of the top-deck about the vertical axis passing through the CM of top-deck. The frequencies ω_{xs}, ω_{ys} and $\omega_{\theta\mathrm{s}}$ are the natural frequencies of the superstructure if it would have torsionally uncoupled i.e. a system with superstructure eccentricity, e_{xs}=0, with m_{s}, K_{xs}, K_{ys} and $K_{\theta\mathrm{s}}$ same as in the torsionally coupled system. Here the eccentricity between the CM of top-deck and the CR of the columns in x-direction is given by

$$e_{\mathrm{xs}} = \frac{1}{K_{\mathrm{ys}}} \sum_i k_{\mathrm{yi}}\ x_{\mathrm{yi}} \tag{4}$$

4. ASYMMETRIES AT THE ISOLATION LEVEL

The CR provided by the isolation system is a resultant of the restoring forces developed in the individual bearings placed below the base-raft. With the differences in isolation stiffness and/ or the yield strength (or friction coefficient) of the individual bearings, the resultant CR of all the bearings does not coincide with the CM of the base-raft. Hence, even when the superstructure is symmetric, due to such isolation eccentricities, the displacement response of the building is affected due to torsional coupling.

Let K_{xbj} and K_{ybj} represent the lateral isolation stiffness and f_{xbj} and f_{ybj} represent the isolation forces in the j^{th} bearing developed in x- and y-directions, respectively. Then

$$K_{\mathrm{xb}} = \sum_j k_{\mathrm{xbj}} \text{ and } K_{\mathrm{yb}} = \sum_j k_{\mathrm{ybj}} \tag{5}$$

are the total lateral stiffness of the isolation system in the x- and y-directions, respectively; whereas the total restoring force component in x- and y-directions F_{xb} and F_{yb} are represented as

$$F_{\mathrm{xb}} = \sum_j f_{\mathrm{xbj}} \text{ and } F_{\mathrm{yb}} = \sum_j f_{\mathrm{ybj}} \tag{6}$$

The torsional force developed due to the isolation system defined about the vertical axis passing through the CM of the base-raft is given by

$$F_{\theta\mathrm{b}} = \sum_j \left(f_{\mathrm{xbj}}\ y_{\mathrm{bj}} + f_{\mathrm{ybj}}\ x_{\mathrm{bj}} \right) \tag{7}$$

where x_{bj} and y_{bj} denote the x- and y- coordinates of the j^{th} bearing with respect to the CM of the base-raft, respectively. The torsional stiffness of the isolation system defined about the vertical axis passing through the CM of the base-raft is given by

$$K_{\theta\mathrm{b}} = \sum_j \left(k_{\mathrm{xbj}}\ y_{\mathrm{bj}}^2 + k_{\mathrm{ybj}}\ x_{\mathrm{bj}}^2 \right) \tag{8}$$

The torsional stiffness of each individual isolation system is negligible hence ignored. The uncoupled frequency parameters of the system are defined as follows

$$\omega_{\mathrm{xb}} = \sqrt{\frac{K_{\mathrm{xb}}}{(m_{\mathrm{s}} + m_{\mathrm{b}})}},\ \omega_{\mathrm{yb}} = \sqrt{\frac{K_{\mathrm{yb}}}{(m_{\mathrm{s}} + m_{\mathrm{b}})}} \text{ and } \omega_{\theta\mathrm{b}} = \sqrt{\frac{K_{\theta\mathrm{b}}}{(m_{\mathrm{s}} + m_{\mathrm{b}}) r_{\mathrm{b}}^2}} \tag{9}$$

where m_{b} and r_{b} are the mass and radius of gyration of the base-raft about the vertical axis through the CM of the base-raft, respectively. The frequencies ω_{xb}, ω_{yb} and $\omega_{\theta\mathrm{b}}$ are the natural frequencies of the isolation system if it would have torsionally uncoupled i.e. a system with isolation eccentricity, e_{xb}=0, with m_{s}, m_{b}, K_{xb}, K_{yb} and $K_{\theta\mathrm{b}}$ same as in the coupled system. In addition, it is to be noted that these frequencies pertain to the rigid superstructure, whereas its mass is duly considered. Here the eccentricity between the CM of base-raft and the CR of the bearings in x-direction is given by

$$e_{\mathrm{xb}} = \frac{1}{K_{\mathrm{yb}}} \sum_j k_{\mathrm{ybj}}\ x_{\mathrm{bj}} + e_{\mathrm{xf}} \tag{10}$$

in which the isolation eccentricity arising due to the differences in the yield strength is separately denoted as

$$e_{\mathrm{xf}} = \frac{1}{F_{\mathrm{yb}}} \sum_{j} f_{\mathrm{ybj}}\, x_{\mathrm{bj}} \tag{11}$$

The isolation eccentricity e_{xb} of CR with respect to CM is developed on account of the dissimilarity in the isolation stiffness amongst the number of isolators placed at different locations below the structure. The isolation eccentricity e_{xf} signifies that the isolators placed at different locations below the structure yielded at different force levels during the earthquake excitation thereby developing an eccentricity of the CR with respect to CM. The total restoring force component in x- and y-directions F_{xb} and F_{yb} are calculated as shown in Eqn 6. The isolation restoring forces developed in the different isolation systems f_{xbj} and f_{ybj} in the j^{th} bearing in x- and y-directions, respectively can be expressed as follows.

4.1. Laminated Rubber Bearings

The popularly used laminated rubber bearings (LRB) comprise of steel and rubber plates built in the alternate layers (Simo and Kelly 1984). The dominant feature of LRB is parallel action of linear spring and damping. Generally, the LRB is characterized with high damping capacity, horizontal flexibility and high vertical stiffness. Schematic diagram of the LRB is shown in Figure 3(a), which represents the linear stiffness with viscous damping. The restoring force developed in the LRB is given by

$$\begin{Bmatrix} f_{\mathrm{xbj}} \\ f_{\mathrm{ybj}} \end{Bmatrix} = \begin{bmatrix} c_{\mathrm{bj}} & 0 \\ 0 & c_{\mathrm{bj}} \end{bmatrix} \begin{Bmatrix} \dot{u}_{\mathrm{xbj}} \\ \dot{u}_{\mathrm{ybj}} \end{Bmatrix} + \begin{bmatrix} k_{\mathrm{bj}} & 0 \\ 0 & k_{\mathrm{bj}} \end{bmatrix} \begin{Bmatrix} u_{\mathrm{xbj}} \\ u_{\mathrm{ybj}} \end{Bmatrix} \tag{12}$$

where $C_{\mathrm{bj}}=C_{\mathrm{xbj}}=C_{\mathrm{ybj}}$ and $K_{\mathrm{bj}}=K_{\mathrm{xbj}}=K_{\mathrm{ybj}}$ are the damping and stiffness of LRB in both x- and y-direction for the j^{th} isolator; and u_{xbj} and u_{ybj} are the relative displacements respectively in x- and y-direction between base-raft and the ground.

The stiffness and damping of the LRB is selected to provide the specific values of the two parameters namely the isolation time period (T_{b}) and damping ratio (ξ_{b}) defined as

$$T_{\mathrm{b}} = 2\pi \sqrt{\frac{(m_{\mathrm{s}} + m_{\mathrm{b}})}{\sum_j k_{\mathrm{bj}}}} \tag{13}$$

$$\xi_{\mathrm{b}} = \frac{\sum_j c_{\mathrm{bj}}}{2(m_{\mathrm{s}} + m_{\mathrm{b}})\omega_{\mathrm{b}}} \tag{14}$$

where $\omega_{\mathrm{b}}=2\pi/T_{\mathrm{b}}$ is the isolation frequency. It is to be noted that the isolation time period, T_{b} in all the directions is the same owing to the orthotropic nature of an individual isolator.

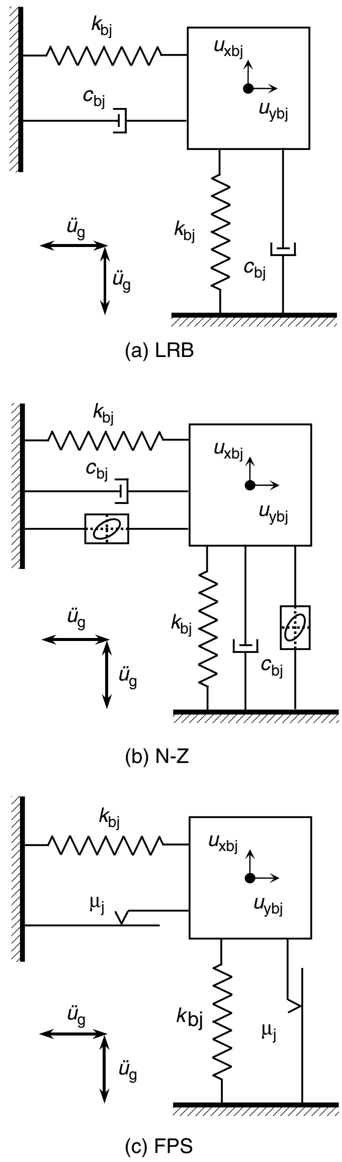

Figure 3. Schematic diagrams of different seismic isolation systems used in the building

4.2. Lead-Rubber Bearings

These bearings are similar to the LRB except that a central lead-core is used to provide an additional means of energy dissipation and initial rigidity against minor earthquakes and winds (Skinner *et al.* 1975; Robinson 1982). These bearings are widely developed and used in New Zealand and are therefore generally referred as N-Z system. The energy absorbing capacity by the lead-core reduces the bearing displacement. The N-Z bearings also provide an additional hysteretic damping through the yielding of lead-core. The force-deformation behavior of the N-Z bearing is generally represented by non-linear characteristics. For the present study, Wen's model

(Wen 1976) is used to characterize the hysteretic behavior of the N-Z bearings, which is shown schematically in Figure 3(b). The restoring force developed in the isolation bearing is given by

$$\begin{Bmatrix} f_{\text{xbj}} \\ f_{\text{ybj}} \end{Bmatrix} = \begin{bmatrix} c_{\text{bj}} & 0 \\ 0 & c_{\text{bj}} \end{bmatrix} \begin{Bmatrix} \dot{u}_{\text{xbj}} \\ \dot{u}_{\text{ybj}} \end{Bmatrix} + \alpha \begin{bmatrix} k_{\text{j}} & 0 \\ 0 & k_{\text{j}} \end{bmatrix} \begin{Bmatrix} u_{\text{xbj}} \\ u_{\text{ybj}} \end{Bmatrix} + (1-\alpha) \begin{bmatrix} f_{\text{j}}^{\text{y}} & 0 \\ 0 & f_{\text{j}}^{\text{y}} \end{bmatrix} \begin{Bmatrix} Z_{\text{xj}} \\ Z_{\text{yj}} \end{Bmatrix} \tag{15}$$

where f_{j}^{y} is the yield strength of the j^{th} bearing in both x- and y-direction; α is an index which represents the ratio of post to pre-yielding stiffness, i.e. $\alpha = k_{\text{bj}}/k_{\text{j}}$; k_{j} is the pre-yield stiffness; and Z_{xj} and Z_{yj} are the non-dimensional hysteretic displacement components satisfying the following non-linear first order differential equations expressed as

$$q_{\text{j}} \begin{Bmatrix} \dfrac{dZ_{\text{xj}}}{dt} \\ \dfrac{dZ_{\text{yj}}}{dt} \end{Bmatrix} = \begin{bmatrix} A - \beta |\dot{u}_{\text{xbj}}| Z_{\text{xj}} |Z_{\text{xj}}| - \tau Z_{\text{xj}}^2 & -\beta |\dot{u}_{\text{ybj}}| Z_{\text{xj}} |Z_{\text{yj}}| - \tau Z_{\text{xj}} Z_{\text{yj}} \\ -\beta |\dot{u}_{\text{xbj}}| Z_{\text{yj}} |Z_{\text{xj}}| - \tau Z_{\text{xj}} Z_{\text{yj}} & A - \beta |\dot{u}_{\text{ybj}}| Z_{\text{yj}} |Z_{\text{yj}}| - \tau Z_{\text{xj}}^2 \end{bmatrix} \begin{Bmatrix} \dot{u}_{\text{xbj}} \\ \dot{u}_{\text{ybj}} \end{Bmatrix} \tag{16}$$

where q_{j} is the yield displacement; the dimensionless parameters β,τ, and A are selected such that predicted response from the model closely matches with the experimental results.

The N-Z system is characterized by the isolation period (T_{b}), damping ratio (ξ_{b}) and the normalized yield strength, i.e. $f_{\text{j}}^{\text{y}}/W$. Here $W=(m_{\text{s}}+m_{\text{b}})g$ is the total weight of the building; and g is the acceleration due to gravity. The isolation parameters T_{b} and ξ_{b} are computed from Eqns 13 and 14, respectively using the post-yield stiffness, k_{bj} of the isolator.

4.3. Friction Pendulum Systems

The concept of sliding systems used along with notion of a pendulum type response, by means of an articulated slider on spherical concave chrome surface, marks a friction pendulum system (FPS) (Zayas *et al.* 1990). The system is activated only when the earthquake forces overcome the static value of friction. The FPS develops a lateral force equal to the combination of the mobilized frictional force and the restoring force that develops because of rising of the structure along the spherical surface. The schematic diagram of FPS is shown in Figure 3(c). The resisting force provided by the system is

$$\begin{Bmatrix} f_{\text{xbj}} \\ f_{\text{ybj}} \end{Bmatrix} = \begin{bmatrix} k_{\text{bj}} & 0 \\ 0 & k_{\text{bj}} \end{bmatrix} \begin{Bmatrix} u_{\text{xbj}} \\ u_{\text{ybj}} \end{Bmatrix} + \begin{Bmatrix} f_{\text{xj}} \\ f_{\text{yj}} \end{Bmatrix} \tag{17}$$

where k_{bj} is the bearing stiffness provided by virtue of inward gravity action at the concave surface; and f_{xj} and f_{yj} are the frictional forces developed in x- and y-directions, respectively.

The system is characterized by the isolation time period (T_{b}) that depends upon radius of curvature of the concave surface and the friction coefficient (μ_{j}). The isolation stiffness, k_{bj} is adjusted such that the specified value of the isolation period evaluated by the Eqn 13 is achieved.

5. GOVERNING EQUATIONS OF MOTION

The torsionally coupled system in consideration has total six degrees-of-freedom, three each at the top-deck and the base-raft. The coupled governing equations of motions at the top-deck and base-raft can be conveniently written separately as follows. The governing equations of motion for the superstructure (top-deck) of the base-isolated system under ground excitation in the x- and y-direction, applied simultaneously considering interaction of the response, are written as

$$\begin{bmatrix} m_{\text{s}} & 0 & 0 \\ 0 & m_{\text{s}} & 0 \\ 0 & 0 & m_{\text{s}} r_{\text{s}}^2 \end{bmatrix} \begin{Bmatrix} \ddot{u}_{\text{xs}} \\ \ddot{u}_{\text{ys}} \\ \ddot{u}_{\theta\text{s}} \end{Bmatrix} + [C] \begin{Bmatrix} \dot{u}_{\text{xs}} \\ \dot{u}_{\text{ys}} \\ \dot{u}_{\theta\text{s}} \end{Bmatrix} + \begin{bmatrix} K_{\text{xs}} & 0 & -K_{\text{xs}} e_{\text{ys}} \\ 0 & K_{\text{ys}} & K_{\text{ys}} e_{\text{xs}} \\ -K_{\text{xs}} e_{\text{ys}} & K_{\text{ys}} e_{\text{xs}} & K_{\theta\text{s}} \end{bmatrix} \begin{Bmatrix} u_{\text{xs}} \\ u_{\text{ys}} \\ u_{\theta\text{s}} \end{Bmatrix} = - \begin{bmatrix} m_{\text{s}} & 0 & 0 \\ 0 & m_{\text{s}} & 0 \\ 0 & 0 & m_{\text{s}} r_{\text{s}}^2 \end{bmatrix} \begin{Bmatrix} \ddot{u}_{\text{xb}} + \ddot{u}_{\text{g}} \\ \ddot{u}_{\text{yb}} + \ddot{u}_{\text{g}} \\ \ddot{u}_{\theta\text{s}} \end{Bmatrix} \tag{18}$$

where $[C]$ is the superstructure damping matrix; $u_{\theta\text{s}} = r_{\text{s}}\theta_{\text{s}}$ is the torsional displacement expressed in terms of the rotation, θ_{s} of the top-deck; and $\ddot{u}_{\text{g}}$ is the same earthquake ground acceleration applied in the two orthogonal directions of the system simultaneously. However, it is to be noted that the torsional coupling occur only between the lateral displacement, u_{yb} and the torsional displacement, $u_{\theta\text{b}}$ as the uni-directional eccentricity, is considered in the x-direction. Here, u_{g} is the absolute ground displacement during the earthquake; u_{xb} and u_{yb} are the displacements of the base-raft relative to the ground respectively in x- and y-directions; and u_{xs} and u_{ys} are the displacements of the top-deck relative to the base-raft respectively in x- and y-directions.

Similarly, the corresponding governing equation of motion can be obtained for the base-raft as follows

$$\begin{bmatrix} m_{\mathrm{b}} & 0 & 0 \\ 0 & m_{\mathrm{b}} & 0 \\ 0 & 0 & m_{\mathrm{b}} r_{\mathrm{b}}^2 \end{bmatrix} \begin{Bmatrix} \ddot{u}_{\mathrm{xb}} \\ \ddot{u}_{\mathrm{yb}} \\ \ddot{u}_{\theta b} \end{Bmatrix} + \begin{Bmatrix} F_{\mathrm{xb}} \\ F_{\mathrm{yb}} \\ F_{\theta \mathrm{b}} \end{Bmatrix} - [C] \begin{Bmatrix} \dot{u}_{\mathrm{xs}} \\ \dot{u}_{\mathrm{ys}} \\ \dot{u}_{\theta \mathrm{s}} \end{Bmatrix} - \begin{bmatrix} K_{\mathrm{xs}} & 0 & -K_{\mathrm{xs}} e_{\mathrm{ys}} \\ 0 & K_{\mathrm{ys}} & K_{\mathrm{ys}} e_{\mathrm{xs}} \\ -K_{\mathrm{xs}} e_{\mathrm{ys}} & K_{\mathrm{ys}} e_{\mathrm{xs}} & K_{\theta \mathrm{s}} \end{bmatrix} \begin{Bmatrix} u_{\mathrm{xs}} \\ u_{\mathrm{ys}} \\ u_{\theta \mathrm{s}} \end{Bmatrix} = - \begin{bmatrix} m_{\mathrm{b}} & 0 & 0 \\ 0 & m_{\mathrm{b}} & 0 \\ 0 & 0 & m_{\mathrm{b}} r_{\mathrm{b}}^2 \end{bmatrix} \begin{Bmatrix} \ddot{u}_{\mathrm{g}} \\ \ddot{u}_{\mathrm{g}} \\ 0 \end{Bmatrix} \tag{19}$$

where $u_{\theta b}=r_b\theta_b$ is the torsional displacement expressed in terms of the rotation, θ_b of the base-raft. The complete system under consideration having six degrees-of-freedom is represented using Eqns 18 and 19 in combination. The presence of the base-raft acceleration terms in Eqn 18 and that of superstructure elastic and damping forces in Eqn 19 shows the interdependence and coupling between top-deck and base-raft. The coupled equations of motion (Eqns 18 and 19) are solved numerically using Newmark's method of step-by-step integration; adopting linear variation of acceleration over a small time interval of Δt.

The system parameters considered for the superstructure eccentricity hence can be summarized as follows

$$\Omega_{\mathrm{s}} = \frac{\omega_{\theta \mathrm{s}}}{\omega_{\mathrm{xs}}} = \frac{\omega_{\theta \mathrm{s}}}{\omega_{\mathrm{ys}}} \tag{20}$$

and that for the isolation eccentricity as follows

$$\Omega_{\mathrm{b}} = \frac{\omega_{\theta b}}{\omega_{\mathrm{xb}}} = \frac{\omega_{\theta b}}{\omega_{\mathrm{yb}}} \tag{21}$$

The two other systems parameters are of eccentricities that are expressed as eccentricity ratios, normalized with the plan dimension, B as e_{xs}/B and e_{xb}/B.

The displacement of the corner bearing is given by

$$u_{\mathrm{c}}(t) = u_{\mathrm{yb}}(t) \pm \frac{B}{2r_{\mathrm{b}}} u_{\theta \mathrm{b}}(t) \tag{22}$$

The UBC (1997) provides following expression for the additional displacement of the bearing due to torsion as

$$D_{\mathrm{TM}} = D_{\mathrm{M}} \left(1 + Y \frac{12e}{B^2 + D^2} \right) \tag{23}$$

where D_{TM} is the total maximum displacement of the bearing; D_M is the maximum displacement at the CR of the bearing; Y is the distance of the corner bearing from the CR; and e is the eccentricity of the system that include the actual plus accidental eccentricity.

6. NUMERICAL STUDY

The objective of this study is to study the different parameters affecting the displacement response of torsionally coupled base-isolated building. The displacement response at the base in the lateral directions, u_{xb}, u_{yb}; torsional displacement, $u_{\theta b}$; and the corner bearing displacement, u_c are investigated under bi-direction earthquake excitation to study the performance of asymmetric base-isolated structure with various isolation systems. The system considered in the present study can be completely characterized by the parameters ω_{xs}, ω_{ys}, ω_{xb}, ω_{yb}, Ω_s, Ω_b, e_{xs}/B, e_{xb}/B and the isolator parameters. However, as the eccentricities are considered only along x-direction, the system parameters limits to ω_{xs}, ω_{xb}, Ω_s, Ω_b, e_{xs}/B, e_{xb}/B along with the isolator parameters. The B/D ratio is kept constant as 1 denoting a square configuration of both the floors of the base-isolated building with mass ratio $m_b/m_s=1$ and the superstructure is assumed to provide the damping ratio of $\xi_s=0.05$. The eccentricity in the system is considered to be 5 percent of the dimension B as specified by the UBC (1997). This implies that the isolated building is designed as symmetric one and the torsion arises only because of the accidental eccentricity in the system. Three earthquake motions selected for the present study are N00E component of 1989 Loma Prieta earthquake recorded at the Los Gatos Presentation Center; N90S component of 1994 Northridge earthquake recorded at the Sylmar station and N00S component of 1995 Kobe earthquake recorded at JMA. The peak ground acceleration (PGA) of Loma Prieta, Northridge and Kobe earthquake motions are 0.57g, 0.6g and 0.86g, respectively. The time interval for solving the coupled equations of motion (Eqns 18 and 19) using these earthquake ground motions is taken as 0.02/20 sec (i.e. Δt = 0.001 sec).

6.1. Effect of Eccentricity due to Isolation Stiffness

In Figures 4, 5 and 6, variation of the peak values of u_{xb}, u_{yb}, $u_{\theta b}$ and u_c against the isolation eccentricity ratio, e_{xb}/B under different earthquakes is plotted keeping $e_{xs}/B = e_{xf}/B = 0$. The frequency ratios are chosen such as $\Omega_s = \Omega_b = 0.8, 1, 1.5$ and 2 representing the torsionally flexible to stiff building, with T_{xs}=0.25sec. The isolation systems utilized here are LRB (T_b=2sec and ξ_b=0.1); N-Z (T_b=2.5sec ξ_b=0.05,q=2.5cm, and f^y/W=0.05) and FPS (T_b=2sec and μ=0.05). The isolation parameters of the N-Z system, as required in Eqn 16, are held constant

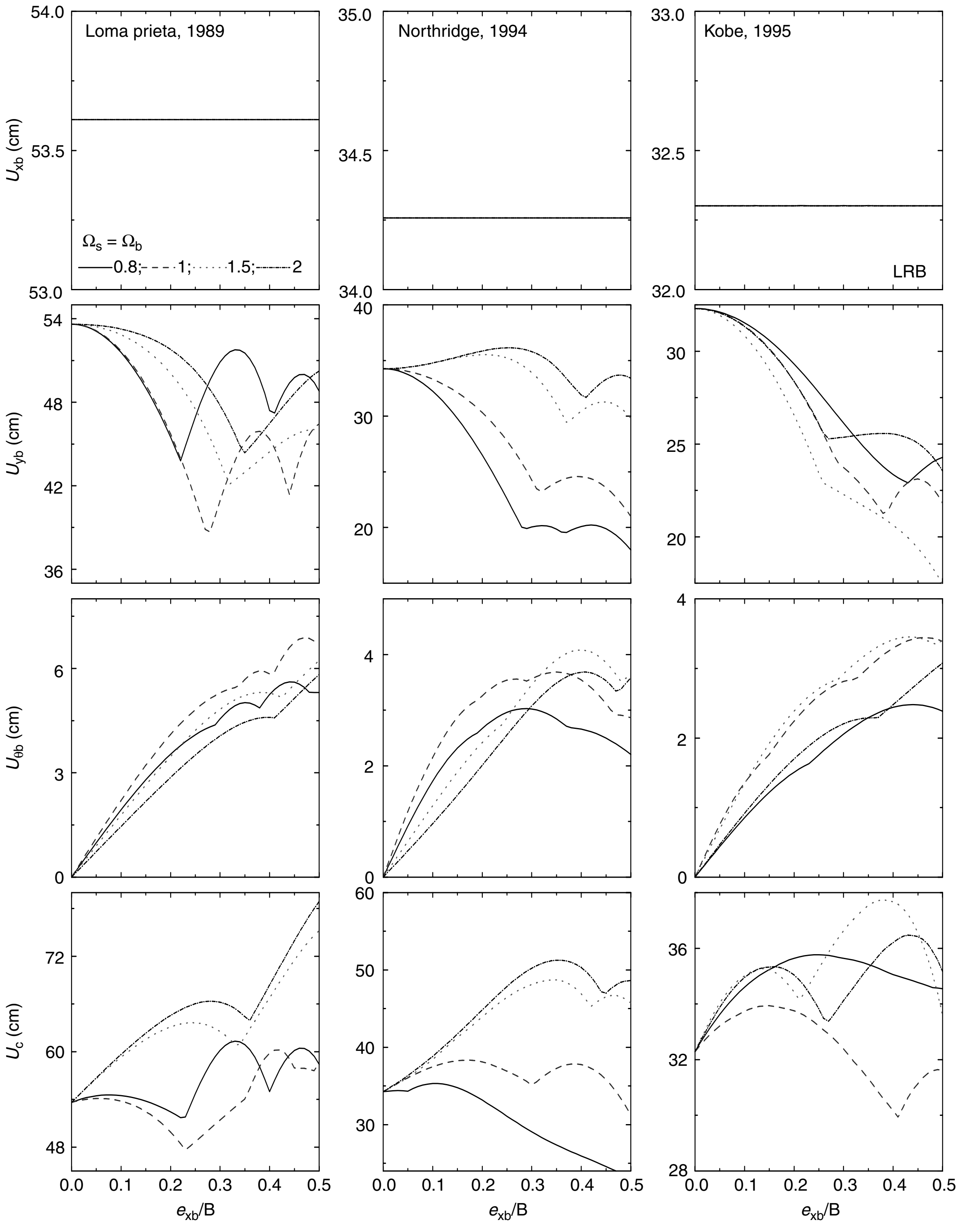

Figure 4. Displacement response of the base-isolated building against the isolation eccentricity ratio due to the isolator stiffness under different earthquakes for LRB

with, β=τ=0.5, A=1 and n=2. It is observed that with the increasing isolation eccentricity, arising due to the differences in the stiffness of the isolators, the lateral displacement reduces and the torsional and corner bearing displacements increases compared to the uncoupled case. Although the system is eccentric only along x-direction, interaction between the lateral displacements, u_{xb} and u_{yb} of the system considered here is reflected from the trend of u_{xb}. The displacement response for FPS amplifies for the torsionally flexible system as compared to that for the LRB and N-Z system.

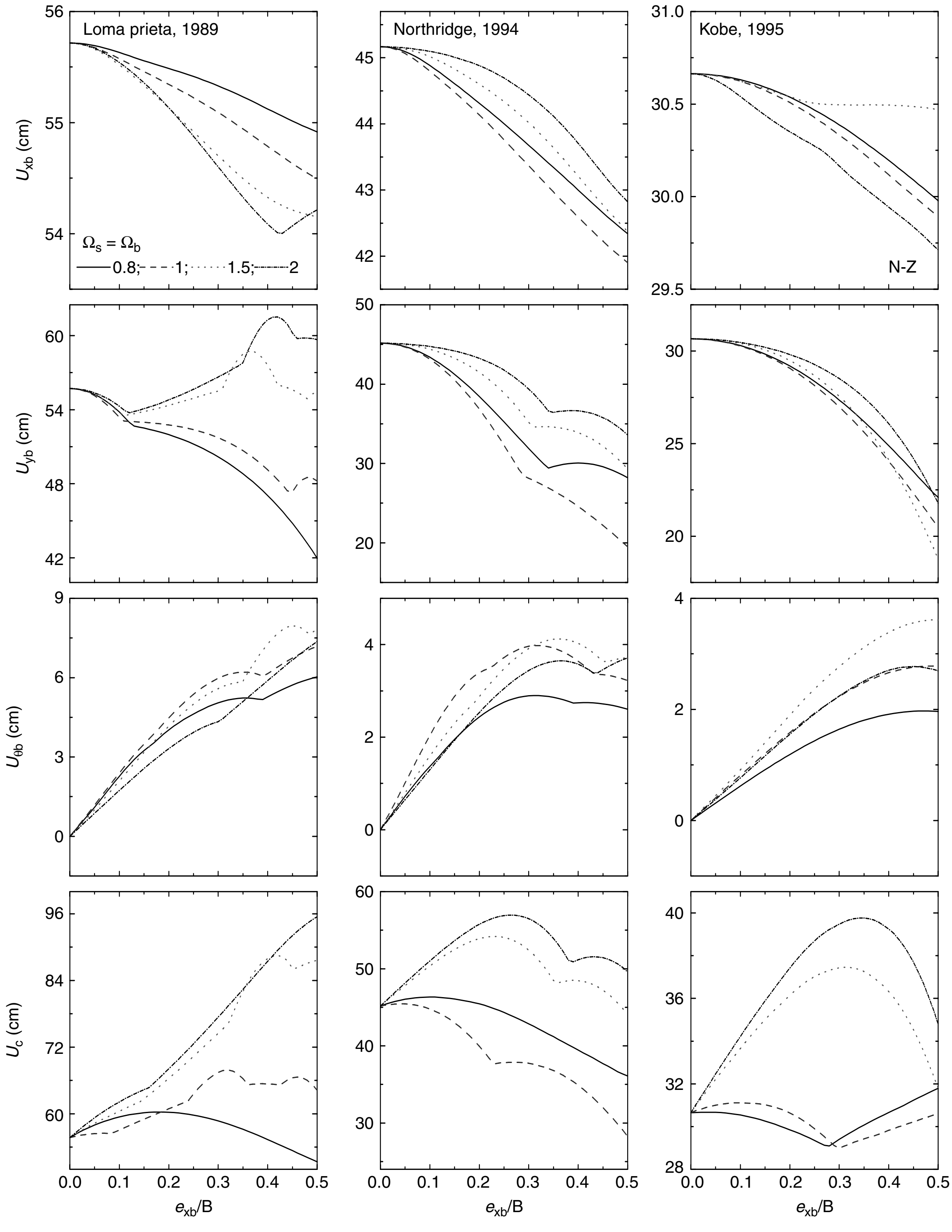

Figure 5. Displacement response of the base-isolated building against the isolation eccentricity ratio due to the isolator stiffness under different earthquakes for N-Z system

6.2. Effect of Eccentricity due to Isolator Yield Strength

The displacement response obtained for Ω_s=Ω_b=0.8, 1, 1.5 and 2 for the isolation eccentricity due to the isolator yield strength is shown in Figures 7 and 8. The variation of the peak values of u_{xb}, u_{yb}, $u_{\theta b}$ and u_c are plotted against the eccentricity ratio, e_{xf}/B, keeping e_{xs}/B=e_{xb}/B=0 under different earthquakes. The isolation systems utilized here are N-Z and FPS with same isolation parameters as defined earlier, with T_{xs}=0.25 sec. It is observed that with the increasing isolation eccentricity, due to differences in yield strength, the displacement in x-direction reduces while that in y-direction increases compared with the uncoupled case. The torsional and

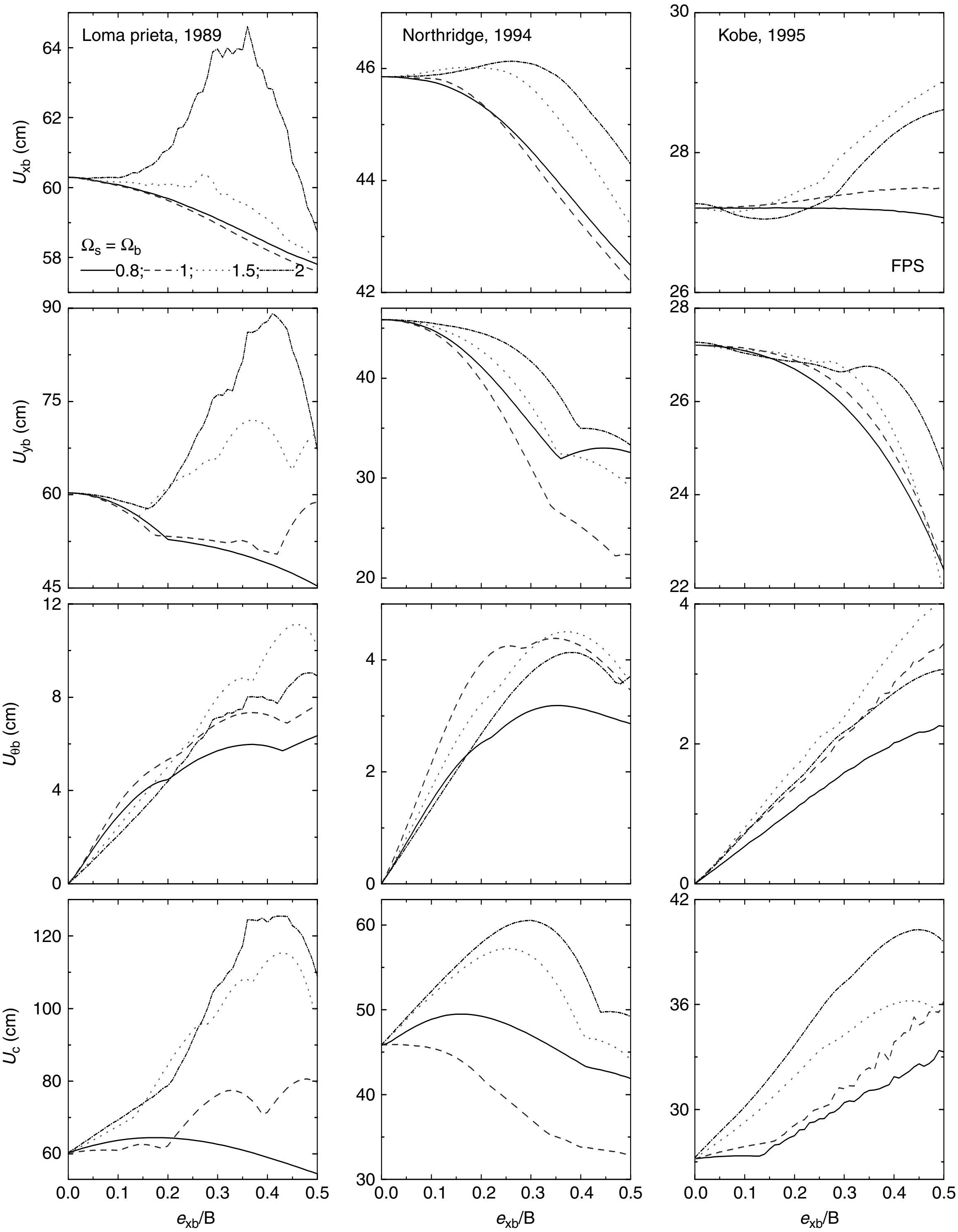

Figure 6. Displacement response of the base-isolated building against the isolation eccentricity ratio due to the isolator stiffness under different earthquakes for FPS

corner bearing displacements are found to increase almost linearly with the increasing isolation eccentricity ratio. From the difference in the displacement response obtained for uncoupled and torsionally coupled systems, it is seen that the N-Z system is more effective compared to the FPS for asymmetric buildings.

6.3. Effect of Superstructure Eccentricity

It is also worthwhile to examine the effects of superstructure eccentricity in presence of the isolation eccentricities. The displacement response obtained for torsionally tuned system, $\Omega_s = \Omega_b = 1$, with $T_{xs} = 0.25$ sec is shown in Table 1 for torsionally coupled base-isolated

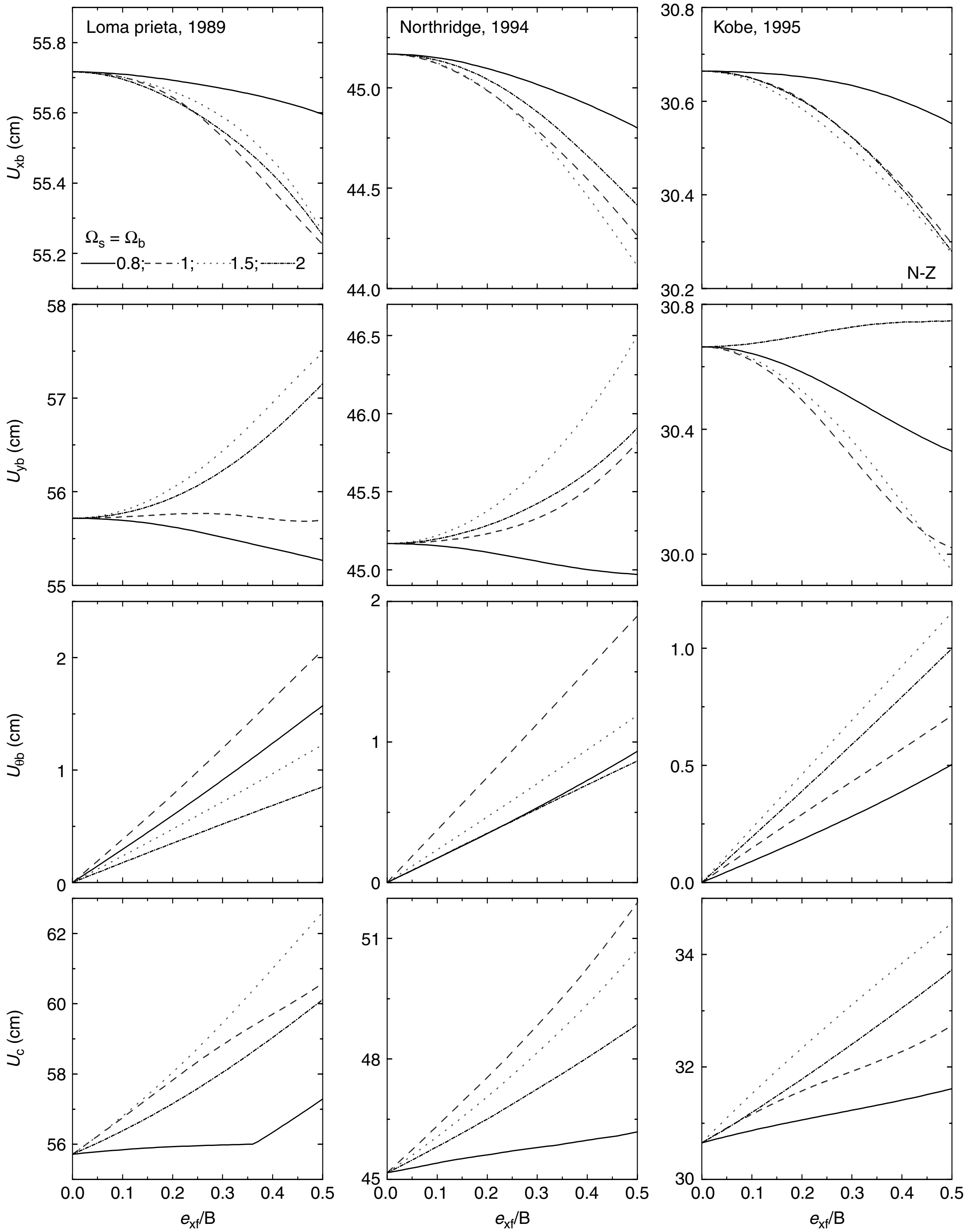

Figure 7. Displacement response of the base-isolated building against the isolation eccentricity ratio due to the isolator yield strength under different earthquakes for N-Z system

building under different earthquakes. The isolation systems namely LRB, N-Z and FPS with similar isolation parameters are chosen when both, the superstructure as well as isolation eccentricities, are present in the structure. The superstructure eccentricity, e_{xs}/B is shown with negative sign implying that its location with respect to the CM is increased towards the opposite direction to that of the isolation eccentricities, e_{xb}/B and e_{xf}/B, while keeping in mind that the CM of the top-deck and base-raft lie on same vertical line.

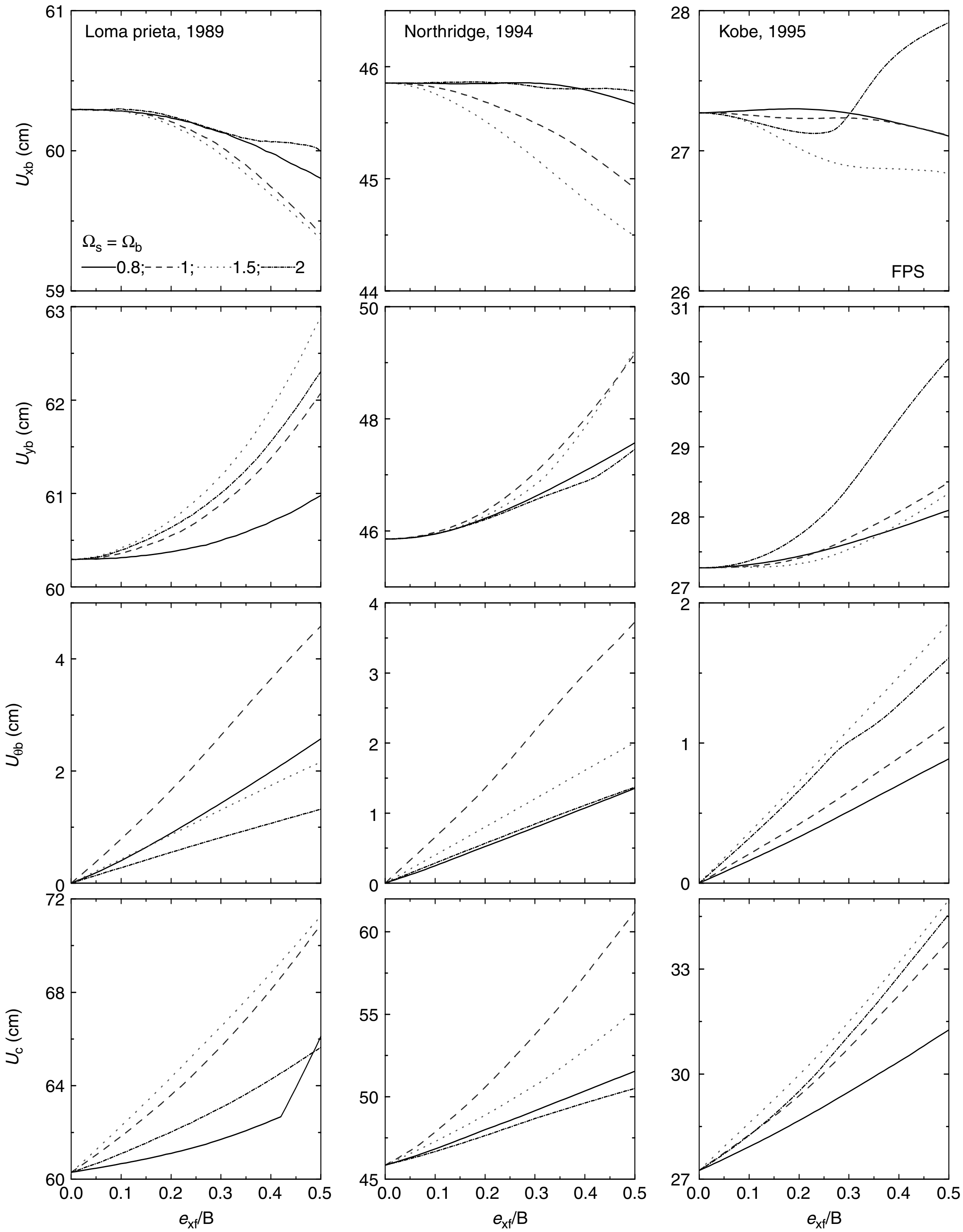

Figure 8. Displacement response of the base-isolated building against the isolation eccentricity ratio due to the isolator yield strength under different earthquakes for FPS

Even after selecting such extreme combination of presence of top-deck and base-raft eccentricities, the displacement response is affected insignificantly. This shows that in presence of the eccentricities due to the isolation parameters, the effects of superstructure eccentricity are negligible on the displacement response. However, when the eccentricities at the superstructure and isolation level falls increasingly on the opposite

Table 1: Displacement response for opposite eccentricities at top-deck and base-raft for tuned case (e_{xb}/B=0.3 and e_{xf}/B=0.3)

Quantity		Loma Prieta, 1989			Northridge, 1994			Kobe, 1995		
Isolators	e_{xs}/B	u_{yb} (cm)	u_c (cm)	$u_{\theta b}$ (cm)	u_{yb} (cm)	u_c (cm)	$u_{\theta b}$ (cm)	u_{yb} (cm)	u_c (cm)	$u_{\theta b}$ (cm)
LRB	0.0	40.9204	51.4089	5.29626	24.2903	35.1113	3.56115	23.7343	32.3851	2.81225
	–0.2	41.0008	51.4257	5.28486	24.3284	35.1342	3.55344	23.7530	32.3602	2.79820
	–0.3	41.0834	51.4392	5.27532	24.3487	35.1484	3.54793	23.7596	32.3151	2.78583
	–0.4	41.2204	51.4633	5.25907	24.3715	35.1661	3.53966	23.7654	32.2262	2.76379
N-Z	0.0	52.6408	76.5477	6.18899	29.7518	41.3887	4.10398	26.0865	29.3956	2.45110
	–0.2	52.5350	76.5013	6.18484	29.7807	41.4095	4.09948	26.1202	29.4248	2.43840
	–0.3	52.4390	76.4607	6.18227	19.7952	41.4170	4.09537	26.1422	29.4382	2.43009
	–0.4	52.3091	76.3865	6.17661	29.8148	41.4230	4.08897	26.1685	29.4523	2.41508
FPS	0.0	61.6061	95.2756	8.22218	30.7777	42.4355	4.57821	25.9517	30.4738	2.31213
	–0.2	61.5365	95.2490	8.21363	30.8703	42.5248	4.58452	25.9808	30.5363	2.30344
	–0.3	61.3889	95.1418	8.19732	30.8620	42.4891	4.57222	26.0106	30.5656	2.29304
	–0.4	61.1584	95.0208	8.18209	30.8808	42.4675	4.55677	26.0466	30.5840	2.28282

direction of the CM at top-deck and base-raft, respectively, the torsional response tends to reduce marginally.

6.4. Effect of Superstructure Flexibility

The parametric study conducted for superstructure eccentricities also invokes interest to observe the effect of superstructure flexibility on the displacement response of torsionally coupled base-isolated buildings. In Figures 9, 10 and 11, variation of the peak values of u_{xb}, u_{yb}, $u_{\theta b}$ and u_c is plotted against the varying superstructure time period, T_{xs} under different earthquakes for LRB, N-Z and FPS, respectively with similar isolation parameters as defined earlier. Other system parameters used are: Ω_s=Ω_b=0.8, 1, 1.5 and 2; e_{xs}/B=0.3; and e_{xb}/B=e_{xf}/B=0. It is observed that with the increasing superstructure flexibility, the lateral displacements reduce and torsional displacements are increased. The increase in torsional displacements is more profound for the torsionally flexible systems.

6.5. Comparison with Code Recommendations

A comparison of the displacement of the corner bearing under different excitations with the corresponding UBC (1997) formula for accidental torsion can be made from Table 2 for LRB, N-Z system and FPS under the three selected earthquake ground motions. The corner bearing displacement, u_c is normalized with the lateral

Table 2: Comparison of normalized corner bearing displacement with UBC (1997) expression for accidental torsion

		Loma Prieta, 1989			Northridge, 1994			Kobe, 1995		
Quantity Isolators	T_b (sec)	Coupled u_c (cm)	Uncoupled u_0 (cm)	u_c/u_0	Coupled u_c (cm)	Uncoupled u_0 (cm)	u_c/u_0	Coupled u_c (cm)	Uncoupled u_0 (cm)	u_c/u_0
LRB	2.0	54.0057	53.6071	1.00744	35.9827	34.2566	1.05039	33.2425	32.3007	1.02916
	2.5	59.0553	57.2026	1.03239	46.5995	47.0498	0.99043	32.2653	31.9910	1.00857
	2.8	71.0567	66.7320	1.06481	48.3805	48.1053	1.00572	33.5962	33.5815	1.00044
N-Z	2.0	57.1822	56.2582	1.01642	34.4881	33.8349	1.01931	36.4446	35.9244	1.01448
	2.5	56.5039	55.7104	1.01424	45.3319	45.1607	1.00379	30.9669	30.6635	1.00989
	2.8	63.2814	61.5628	1.02792	44.5807	44.3246	1.00578	31.3906	31.5032	0.99643
FPS	2.0	59.9833	59.1599	1.01392	41.2199	40.8345	1.00944	35.7778	35.3922	1.0109
	2.5	60.8035	60.0146	1.01315	45.9328	45.8483	1.00184	27.6084	27.2721	1.01233
	2.8	74.7888	75.8269	0.98631	44.8085	44.5558	1.00567	29.0016	28.7967	1.00712

Normalized corner bearing displacement using UBC (1997) expression (Eq. 23) for accidental torsion = 1.14.

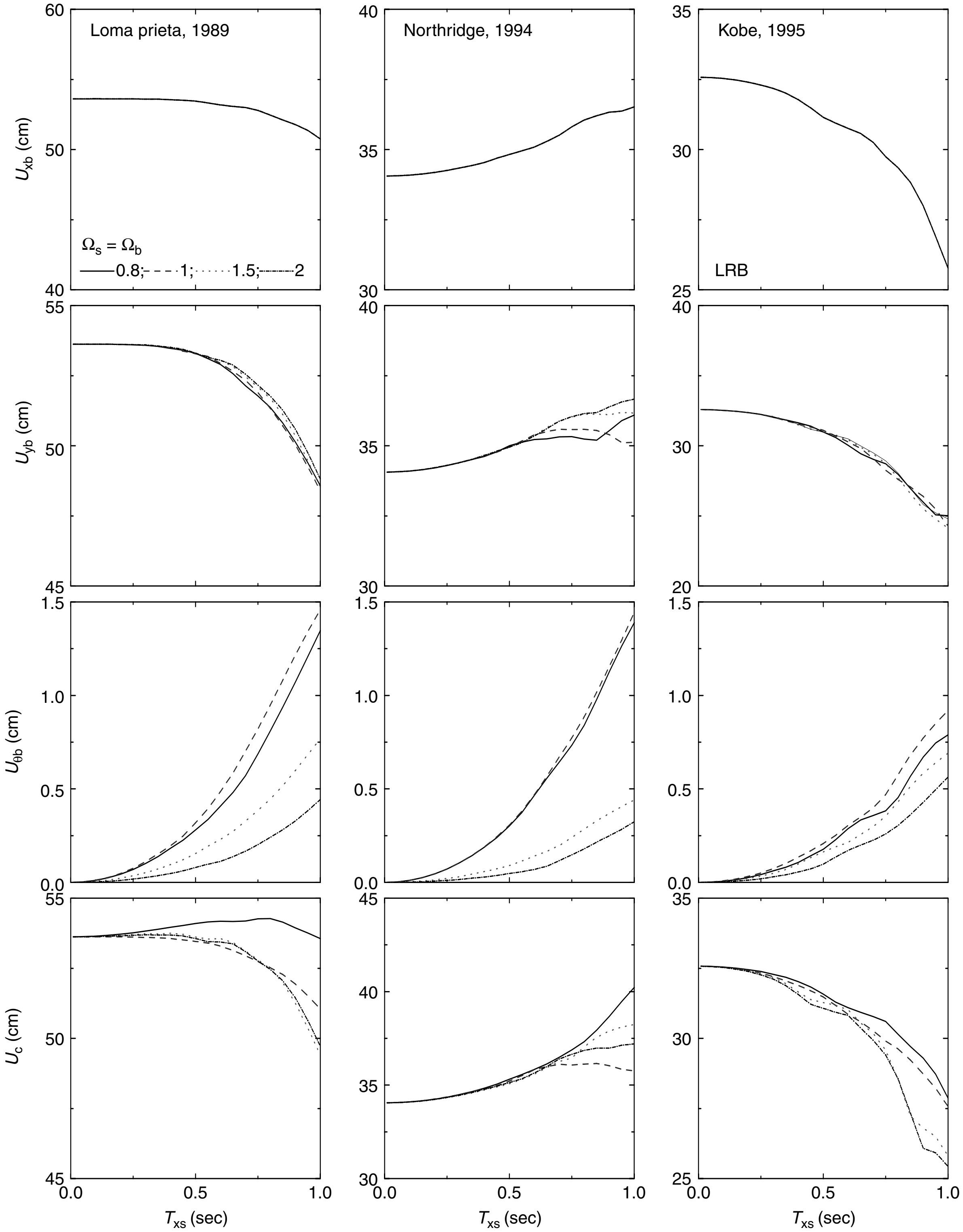

Figure 9. Effect of superstructure flexibility on the displacement response of the base-isolated building with LRB under different earhquakes

displacement of the torsionally uncoupled structure, u_0. As specified by the UBC (1997), the isolation eccentricity of $e_{xb}=0.05B$ is considered with $e_{xs}/B= e_{xf}/B=0$ and the isolation parameters are kept same as previous for torsionally tuned system ($\Omega_s=\Omega_b=1$), with $T_{xs}=0.25$sec. The normalized corner bearing displacement using UBC (1997) expression (Eqn 23) for accidental torsion is 1.14 for the present system. It is

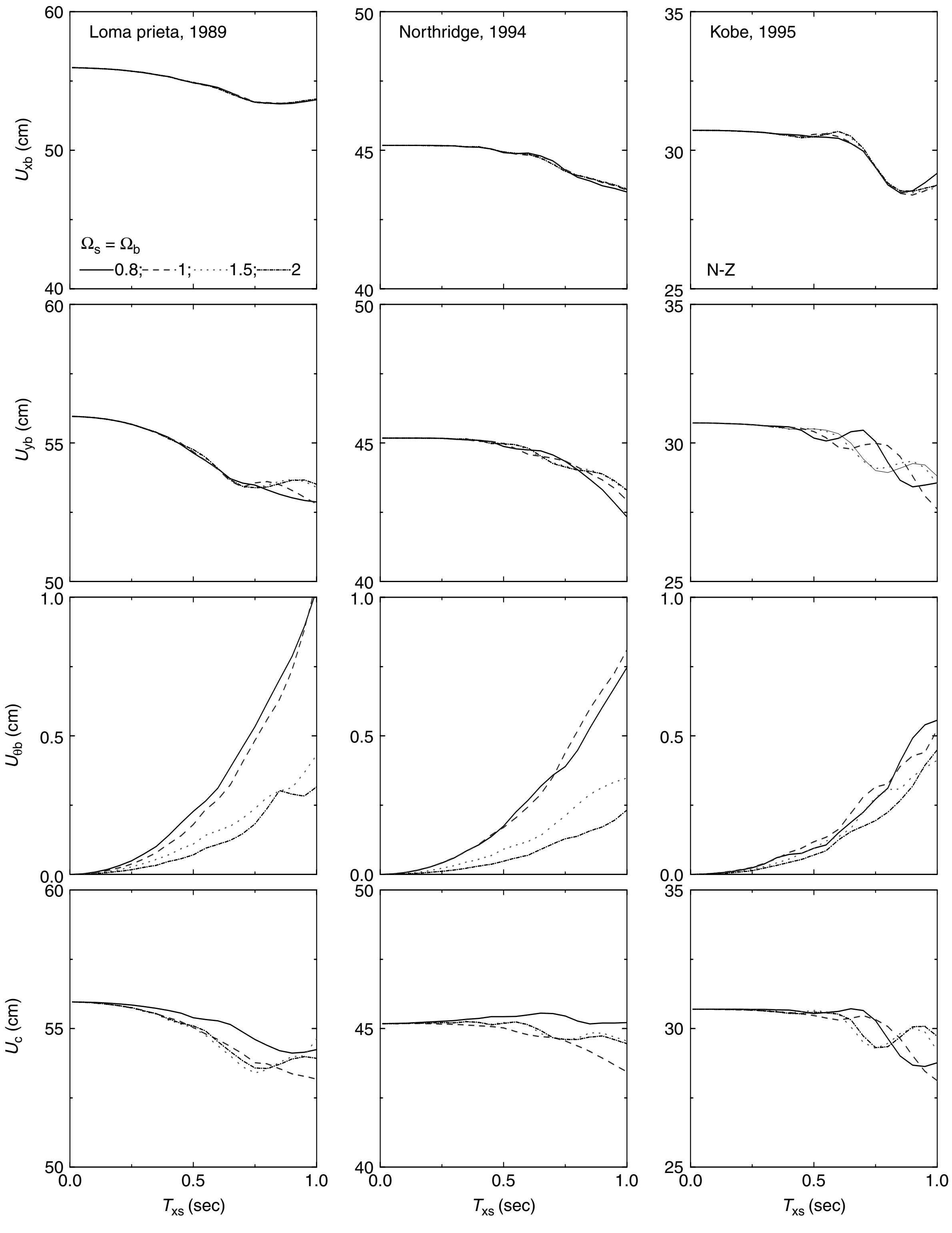

Figure 10. Effect of superstructure flexibility on the displacement response of the base-isolated building with N-Z system under different earthquakes

seen that the displacement of the corner bearing is overestimated by the UBC expression in all cases for the base-isolated buildings torsionally coupled due to the dissimilar isolator parameters.

7. CONCLUSIONS

The effects of torsional coupling, due to the isolator parameters, on the seismic response of base-isolated buildings are studied here. Following conclusions can

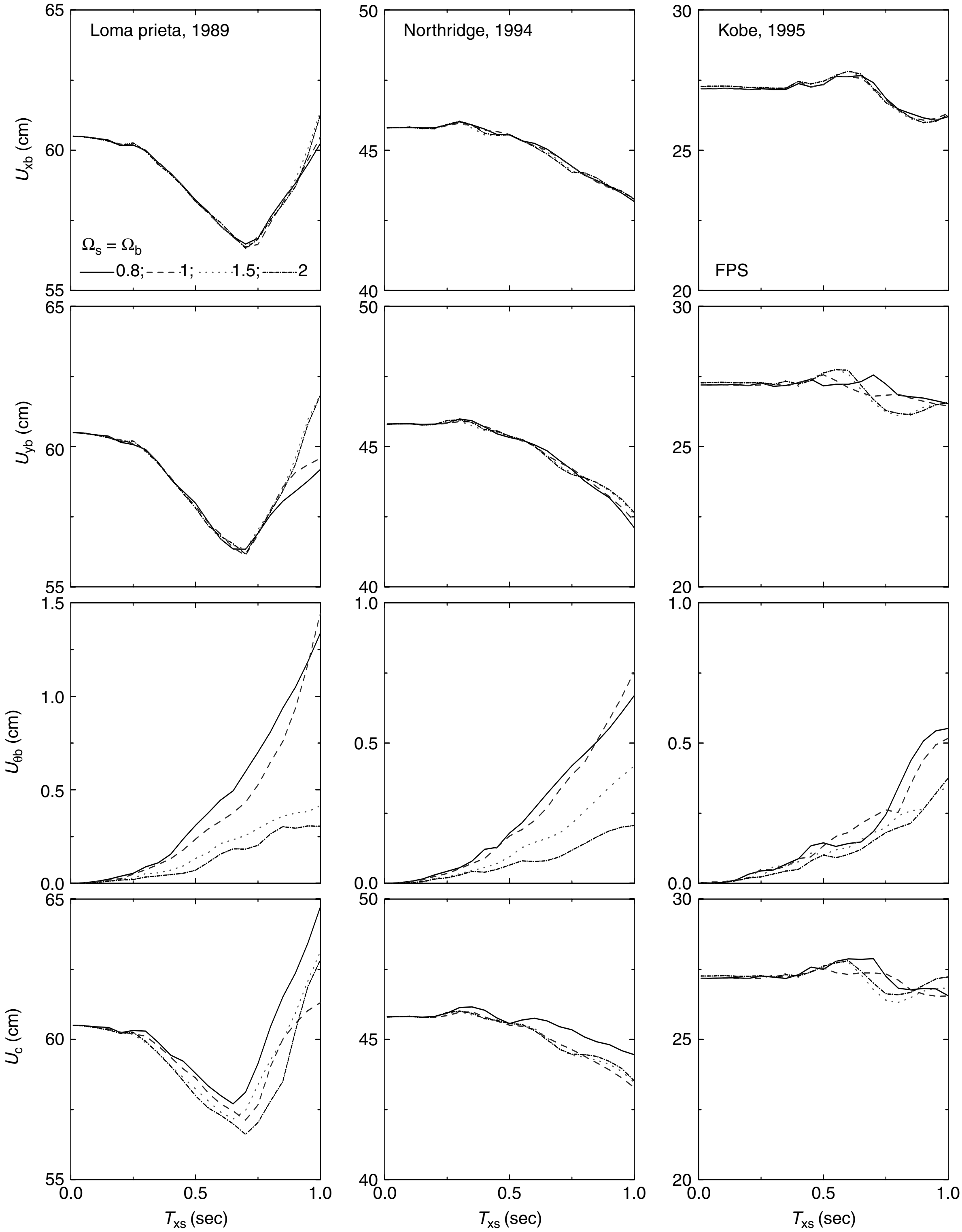

Figure 11. Effect of superstructure flexibility on the displacement response of the base-isolated building with FPS under different earthquakes

be arrived at from the study of displacement response of torsionally coupled base-isolated building subjected to horizontal component of earthquake ground motion.

1. The eccentricities arising due to the dissimilar isolator properties (isolation stiffness and/ or yield strength) in the base-isolated building have major influence on the displacement response and in presence of such isolation eccentricities, the superstructure eccentricity is unimportant;

2. For torsionally flexible system, the displacement response is more than that in case of the torsionally rigid system. In case of torsionally tuned systems, the displacement response is the minimum;
3. In the flexible superstructure of the asymmetric base-isolated building, the lateral displacements reduce and the torsional displacement increases. The increase in torsional displacements is more profound for the torsionally flexible systems;
4. The UBC (1997) formula for accidental torsion over-estimates the design displacements in the base-isolated building with eccentricities arising due to the isolator parameters.

REFERENCES

Eisenberger, M. and Rutenberg, A. (1986). "Seismic base isolation of asymmetric shear buildings", *Engineering Structures*, Vol. 8, No. 1, pp. 2–8.

Gavin, H., Alhan, C. and Oka, N. (2003). "Fault tolerance of semi-active seismic isolation", *Journal of Structural Engineering*, ASCE, Vol. 129, No. 7, pp. 922–932.

IBC (2000). *International Building Code*, International Code Council, USA.

Jangid, R.S. (1996). "Seismic response of an asymmetric base-isolated structure", *Computers and Structures*, Vol. 60, No. 2, pp. 261–267.

Jangid, R.S. and Datta, T.K. (1994a). "Non-linear response of torsionally coupled base-isolated structure", *Journal of Structural Engineering,* ASCE, Vol. 120, No. 1, pp. 1–22.

Jangid, R.S. and Datta, T.K. (1994b). "Seismic response of torsionally coupled structure with elasto-plastic base isolation", *Engineering Structures*, Vol. 16, No. 4, pp. 256–262.

Jangid, R.S. and Datta, T.K. (1995a). "Seismic behaviour of base-isolated buildings: a state-of-the-art review", *Structures and Buildings*, Vol. 110, No. 2, pp. 186–203.

Jangid, R.S. and Datta, T.K. (1995b). "Performance of base isolation systems for asymmetric building subject to random excitation", *Engineering Structures*, Vol. 17, No. 6, pp. 443–454.

Jangid, R.S. and Datta, T.K. (1995c). "The stochastic response of asymmetric base-isolated buildings", *Journal of Sound and Vibration*, Vol. 179, No. 3, pp. 463–473.

Kelly, J.M. (1986). "Aseismic base isolation: a review and bibliography", *Soil Dynamics and Earthquake Engineering*, Vol. 5, No. 4, pp. 202–216.

Lee, D.M. (1980). "Base isolation for torsion reduction in asymmetric structures under earthquake loading", *Earthquake Engineering and Structural Dynamics*, Vol. 8, No. 4, pp. 349–359.

Nagarajaiah, S., Reinhorn, A.M. and Constantinou, M.C. (1991). "Non-linear dynamic analysis of 3-D base-isolated structures", *Journal of Structural Engineering*, ASCE, Vol. 117, No. 7, pp. 2035–2054.

Nagarajaiah, S., Reinhorn, A.M. and Constantinou, M.C. (1993a). "Torsional coupling in sliding base-isolated structures", *Journal of Structural Engineering*, ASCE, Vol. 119, No. 1, pp. 130–149.

Nagarajaiah, S., Reinhorn, A.M. and Constantinou, M.C. (1993b). "Torsion in base-isolated structures with elastomeric isolation systems", *Journal of Structural Engineering*, ASCE, Vol. 119, No. 10, pp. 2932–2951.

Pan, T.C. and Kelly, J.M. (1983). "Seismic response of torsionally coupled base-isolated structures", *Earthquake Engineering and Structural Dynamics*, Vol. 11, No. 6, pp. 749–770.

Reinhorn, A., Constantinou, M. and Nagarajaiah, S. (1994). "3D-basis: computer program series for non-linear dynamic analysis of three-dimensional base-isolated structures", *The National Center for Earthquake Engineering Research (NCEER)*, pp. 41–54.

Robinson, W.H. (1982). "Lead rubber hysteretic bearings suitable for protecting structures during earthquakes", *Earthquake Engineering and Structural Dynamics*, Vol. 10, pp. 593–604.

Ryan, K.L. and Chopra, A.K. (2002). "Approximate analysis methods for asymmetric plan base-isolated buildings", *Earthquake Engineering and Structural Dynamics*, Vol. 31, No. 1, pp. 33–54.

Ryan, K.L. and Chopra, A.K. (2004). "Estimation of seismic demands on isolators in asymmetric buildings using non-linear analysis", *Earthquake Engineering and Structural Dynamics*, Vol. 33, No. 3, pp. 395–418.

Simo, J.C. and Kelly, J.M. (1984). "The analysis of multi-layer elastomeric bearings", *Journal of Applied Mechanics*, ASME, Vol. 51, pp. 256–262.

Skinner, R.I., Kelly, J.M. and Heine, A.J. (1975). "Hysteretic dampers for earthquake-resistant structures", *Earthquake Engineering and Structural Dynamics*, Vol. 3, No. 3, pp. 287–296.

Tena-Colunga, A. and Gomez-Soberon, C. (2002). "Torsional response of base-isolated structures due to asymmetries in the superstructure", *Engineering Structures*, Vol. 24, No. 12, pp. 1587–1599.

Tena-Colunga, A., Gomez-Soberon, C. and Munoz-Loustanau, A. (1997). "Seismic isolation of buildings subjected to typical subduction earthquake motions for the mexican pacific coast", *Earthquake Spectra*, Vol. 13, No. 3, pp. 505–532.

Tsopelas, P.C., Nagarajaiah, S., Constantinou, M.C. and Reinhorn, A.M. (1994). "Non-linear dynamic analysis of multiple building base isolated structures", *Computers and Structures*, Vol. 50, No. 1, pp. 47–57.

UBC (1997). *Uniform Building Code*, International Conference of Building Officials, Whittier, California.

Wen, Y.K. (1976). "Method for random vibrations of hysteretic systems", *Journal of the Engineering Mechanics Division*, ASCE, Vol. 102, No. 2, pp. 249–263.

Zayas, V.A., Low, S.S. and Mahin, S.A. (1990). "A simple pendulum technique for achieving seismic isolation", *Earthquake Spectra*, Vol. 6, No. 2, pp. 317–333.

APPENDIX: NOTATION

μ	= Coefficient of friction in the sliding systems
α	= Index of the ratio of isolator post to pre-yield stiffness
β, τ, A and n	= Dimensionless Wen's parameters
ξ_b	= Isolation damping ratio
ξ_s	= Superstructure damping ratio
Ω_b	= Isolation frequency ratio
Ω_s	= Superstructure frequency ratio
θ_b	= Rotation of the base-raft
θ_s	= Rotation of the top-deck
Δt	= A small time interval
ω_{xb}, ω_{yb}, $\omega_{\theta b}$	= Uncoupled isolation frequencies
ω_{xs}, ω_{ys}, $\omega_{(s}$	= Uncoupled superstructure frequencies
$[C]$	= Damping matrix
B, D	= Plan dimensions of top-deck and base-raft
c_{bj}, c_{xbj}, c_{ybj}	= Isolation damping
D_M	= Maximum bearing displacement
D_{TM}	= Total maximum bearing displacement
e	= Total eccentricity
e_{xb}	= Isolation eccentricity due to stiffness
e_{xf}	= Isolation eccentricity due to yield strength
e_{xs}	= Superstructure eccentricity
F_{xb}, F_{yb}	= Total isolation restoring forces
$F_{\theta b}$	= Torsional isolation forces
f_{xbj}, f_{ybj}	= Isolation forces
f^y	= Isolator yield force
f_{xj}, f_{yj}	= Frictional force
g	= Acceleration due to gravity
k_j	= Isolator pre-yield stiffness
k_{bj}	= Isolator post-yield stiffness
$K_{\theta b}$	= Torsional isolation stiffness
$K_{\theta s}$	= Total torsional superstructure stiffness
$k_{\theta s}$	= Torsional superstructure stiffness
K_{xb}, K_{yb}	= Total lateral isolation stiffness
k_{xbj}, k_{ybj}	= Lateral isolation stiffness
k_{xi}, k_{yi}	= Lateral superstructure stiffness
K_{xs}, K_{ys}	= Total lateral superstructure stiffness
m_b	= Mass of the base-raft
m_s	= Mass of the top-deck
q	= Isolator yield displacement
r_b	= Radius of gyration of the base-raft
r_s	= Radius of gyration of the top-deck
T_b	= Isolation time period
T_{xs}	= Superstructure time period
u_0	= Lateral displacement of the torsionally uncoupled structure
u_θ	= Torsional displacement
$u_{\theta b}$	= Torsional displacement of the base-raft
$u_{\theta s}$	= Torsional displacement of the top-deck
u_c	= Corner bearing displacement
u_x	= Lateral displacement in x-direction
u_{xb}, u_{yb}	= Relative displacements of base-raft
u_y	= Lateral displacement in y-direction
W	= Total weight of the building
x_{bj}, y_{bj}	= Coordinates of bearings in x- and y-direction
x_i, y_i	= Coordinates of columns in x- and y-direction
Y	= Distance of the corner bearing from the CR
Z_x, Z_y	= Non-dimensional hysteretic displacement components
u_g, $\ddot{u}_g$	= Earthquake ground displacement and acceleration

Mr. Vasant A. Matsagar is presently a doctoral student at the Department of Civil Engineering at Indian Institute of Technology Bombay, India. After graduating from the Government College of Engineering, Aurangabad, India, in 1997 he obtained his Masters degree in Structural Engineering from the University of Pune, India in 1998. His present area of research includes the aseismic design of structures using passive seismic control devices and its implementation to the real-life structures. He has three years field experience in the analysis and design of structures. He received the 'Young Professional Award' conferred by the Institution of Engineers (India) in 2004.

Dr. R.S. Jangid is associate professor at the Department of Civil Engineering at Indian Institute of Technology Bombay, India. He received B.E. (Hons.) in Civil Engineering from the University of Jodhpur, India in 1989, and his M.Tech. and Ph.D. in Structural Engineering from Indian Institute of Technology Delhi, India in 1991 and 1993, respectively. His research interest includes the aseismic design of structures using active and passive control devices and the dynamic analysis of non-classically damped systems. His recent research contribution includes the base isolation for near-fault motions and its application to the bridges and tanks, multiple tuned mass dampers for vibration control and active control of torsionally coupled structures. He received the 'Young Engineer Award' of the Indian National Academy of Engineering in 1998 for his significant contribution towards research in the area of earthquake engineering and awarded with the 'BOYSCAST fellowship' of the Department Science and Technology, India.

Advances in Structural Engineering, *An International Journal*

website: http://www.cse.polyu.edu.hk/jase/jase.htm

All subscription and further information available from:
Multi-Science Publishing Co. Ltd., 5 Wates Way, Brentwood, Essex CM15 9TB, UK
Tel: +44 (0)1277 224632   Fax: +44 (0)1277 223453
e-mail: mscience@globalnet.co.uk   www.multi-science.co.uk

Aims and Scope of the Journal

Advances in Structural Engineering aims to provide a major publication channel for research in the general area of structural engineering, an international forum for the exchange of innovative ideas, and a conduit for the flow of information between the West and the East, particularly China. Especially welcome are papers describing research directed at the solution of the real engineering problems which arise in challenging construction projects. As well as full length papers, short technical notes, discussions, book reviews and conference reports, are also published. In addition, the journal publishes short articles introducing to readers selected researchers and research institutions in China. Acceptance of a paper for publication in the journal is subject to the manuscript being an unpublished work presenting a significant original contribution or an in-depth state-of-the-art review of a specific topic in structural engineering.

Instructions for Authors

Submission of Papers

Electronic submission of papers is preferred by the journal as it can speed up the review and publication process. Authors should email their manuscripts as PDF files to the Editor-in-Chief, Professor J. G. Teng (cejgteng@polyu.edu.hk). The final revised version of a paper should be emailed to the Editor-in-Chief both as a PDF file and as an MS Word file.

Submission of hard copies of papers is also acceptable. Four copies of a manuscript should be submitted to the Editor-in-Chief, Professor J. G. Teng, Department of Civil and Structural Engineering, The Hong Kong Polytechnic University, Hong Kong, China.

Acceptance of a paper for publication in the journal is subject to the manuscript being an unpublished work presenting a significant original contribution or an in-depth state-of-the-art review of a specific topic in structural engineering. Submission of a manuscript is taken to imply that it is not being considered for publication elsewhere. The submission of a manuscript is also taken to imply that the author(s) agree(s) to cede the copyright of the paper to the publisher of the journal upon its acceptance for publication, but will retain certain rights over the use of the material presented in the paper in their future publications in accordance with common practices of international scientific journals.

Review Process

All papers submitted will be rigorously reviewed by at least two international experts. When a paper is returned for revision prior to final acceptance, the revised version must be submitted within 3 months of the authors' receipt of the referees' reports.

Manuscript Preparation

The manuscript should be provided in double-spaced typing on A4 size pages. It must be written in English and should not, normally, exceed 10,000 word-equivalents. Technical notes should not exceed 3,000 word-equivalents. The title should be concise and be followed by the name(s) and affiliation(s) of the author(s). The main body of the paper is to be preceded by an abstract of about 150 words, reporting concisely on the objectives and conclusions, and a list of 4 to 8 keywords. The contact details of the corresponding author including telephone and fax numbers as well as email address should be provided in a footnote on the first page. Other footnotes are to be avoided. The metric system is to be used throughout and if it is necessary to quote other units then these should be added in parentheses.

The manuscript is expected to be written in correct and easily readable English. Both English and American spellings are acceptable, but each paper is expected to follow one style consistently.

When referring to figure numbers, please use Figure in full, followed by the number. When referring to equation numbers, the word equation and equations should be abbreviated to Eqn and Eqns, respectively. Thus, one may write: "… the figure on the left relates to Eqn 32 and the figures on the right relate to Eqns 33 to 37. Eqns 38 and 39, on the other hand, relate to Figures 102 and 103, respectively. Figure 102 is seen to be similar to Figure 103(a) but the two figures have clear differences that reflect the differences in their equations…"

Symbols denoting matrices and vectors may appear in two different styles:

(1) The symbols may appear enclosed in square brackets (for matrices) or curly brackets (for vectors).

(2) The symbols are preferred in roman, but may appear in bold face where they have been used before but in a different context. To signify this, the symbols must be bold-faced or a note should appear in the margin where they are to be bold face.

Each paper is expected to follow one of these styles consistently.

References

References to published work should be referred to in the text by the last name(s) of author(s) followed by the year of publication in parentheses. For example, one may write "Smith et al. (1996) referred to several existing studies (Chen 1990, 1991, 1992a,b; Ko et al. 1992; Zhu and Ko 1995)…" or "More information can be found in Livesley (1975)." The references should be grouped at the end of the paper in the alphabetical order of the last name of the first author in the following style:

Ko, J.M., Ni, Y.Q. and Tian, Q.L. (1992). "Hysteretic behavior and empirical modelling of a wire-cable vibration isolator", *International Journal of Analytical and Experimental Modal Analysis*, Vol. 7, No. 2, pp. 111–127.

Ko, J.M. and Xu, Y.L., eds, (2000). *Proceedings of International Conference on Advances in Structural Dynamics*, Hong Kong, China, December.

Teng, J.G., Chen, J.F., Smith, S.T. and Lam, L. (2002). *FRP-Strengthened RC Structures*, John Wiley and Sons, Chichester, UK.

Anson, M. and Zhang, J.P. (1995). "On-site graphics for planning and communicating the use of site space", *Proceedings of the Fifth East Asia-Pacific Conference on Structural Engineering and Construction*, Y.C. Loo, ed., Griffith University, Gold Coast, Australia, July, pp. 883–888.

Ho, W.M.G. (1991). *Nonlinear Analysis of Steel Frames with Semi-Rigid Connections*, PhD Thesis, The Hong Kong Polytechnic University, Hong Kong, China.

Illustrations

The original or electronic file of each illustration must be provided with the final revised submission. Each illustration must be clearly numbered. Illustrations should be separated from the text and attached to the end of the text. Captions for the illustrations should be typed in numerical order and placed at the end of the manuscript. The illustrations should preferably require the same degree of reduction. The type area of the journal is 175mm wide and 250mm deep, in two columns per page, each 85mm wide, and lettering should be large enough to be legible after reduction of the illustration to fit the page or column width. Hand-written lettering is not acceptable.

Proofs

Authors will receive proofs which should be corrected and returned without delay. No new material may be inserted in the text at the time of proof reading. All joint papers must indicate the name and full postal address of the author to whom proofs should be sent.

Page Charges and Offprints

There will be no page charges. The publisher will e-mail a PDF copy of the article to the corresponding author. Additional copies can be ordered at current printing prices.